Miniaturized platform with on-chip strain sensors for compression testing of arrayed materials

Luke MacQueen,[a] Oleg Chebotarev,[ab] Craig Simmons,[*abc] and Yu Sun [*ab]

[a]*Department of Mechanical and Industrial Engineering, University of Toronto, 5 King's College Road, Toronto, Ontario, Canada M5S 3G8. E-mail: simmons@mie.utoronto.ca; sun@mie.utoronto.ca; Fax: +1 416 978 7753; Tel: +1 416 946 0548; +1 416 946 0549*
[b]*Institute of Biomaterials and Biomedical Engineering, University of Toronto, 164 College Street, Toronto, Ontario, Canada M5S 3G9*
[c]*Faculty of Dentistry, University of Toronto, 124 Edward Street, Toronto, Ontario, Canada M5G 1G6*

Supplementary Figures

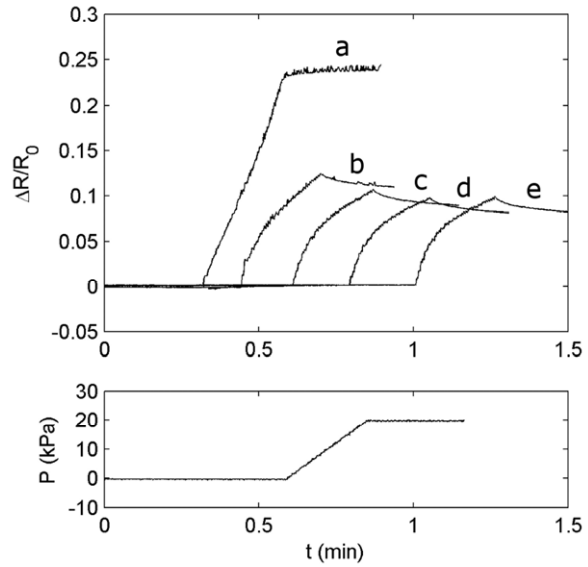

Fig. S1 Strain sensor signal conditioning. Time-dependent resistive strain, $\Delta R/R_0$, of a strain sensor (top panel): Curves a-e are independent measurements performed on days 1-5, respectively, in all cases using the driving pressure, P, shown in the bottom panel.

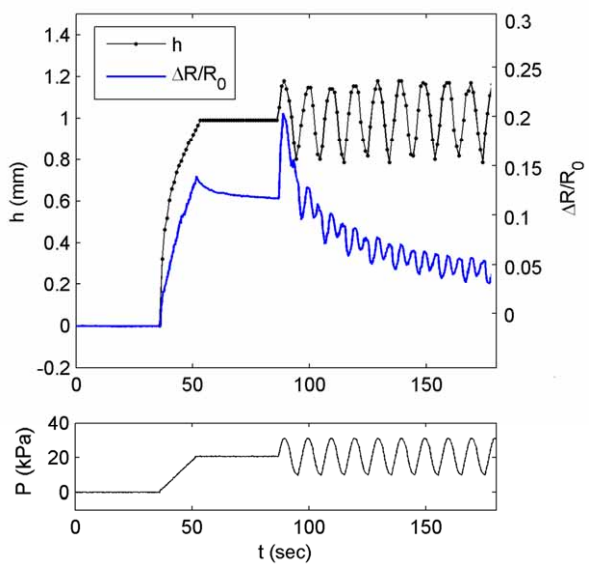

Fig. S2 Membrane height and corresponding strain sensor signal. Membrane height, h, measured optically, and corresponding strain sensor signal, $\Delta R/R_0$, resulting from the driving pressure, P, shown in the bottom panel.

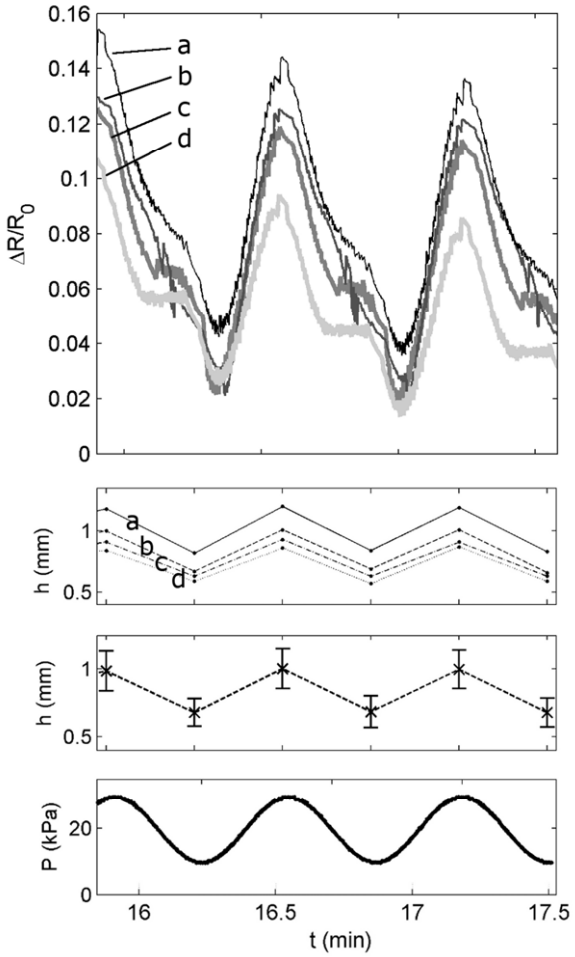

Fig. S3 Strain sensor signal and membrane deflection amplitude resulting from cyclic driving pressure. Time-dependent resistive strain, $\Delta R/R_0$, of four sensors (top panel, a-d); maximum membrane deflection amplitude, h, of four independent membranes (second panel from top, a-d), their mean ± SD (third panel from top), and the corresponding driving pressure, P (bottom panel); P was the same for all panels.

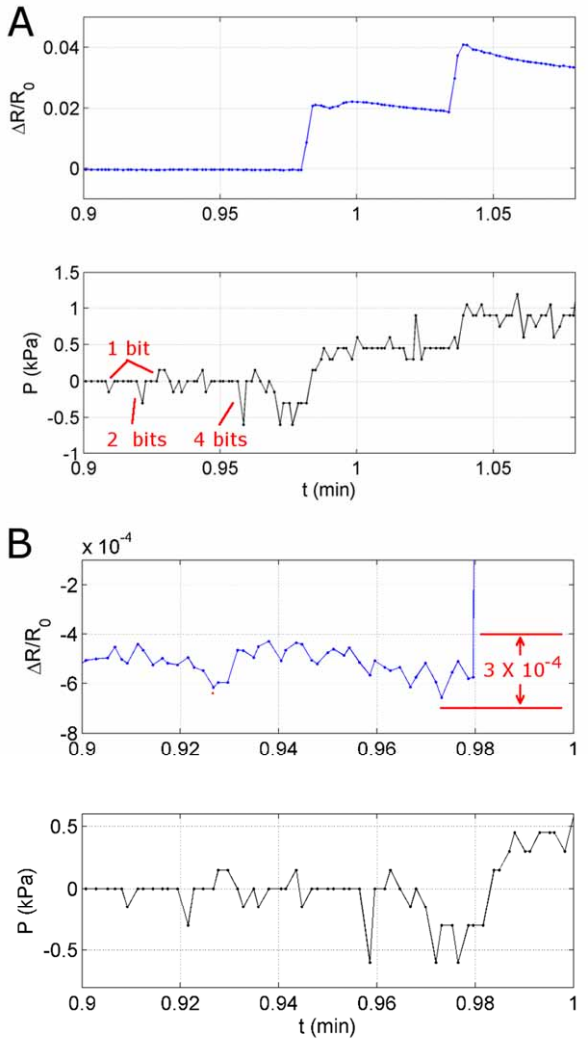

Fig. S4 Resolution of CNT:PDMS strain sensors. (A) Smooth changes in resistive strain, $\Delta R/R_0$ (top panel), contrasted with digital noise in pressure, P (bottom panel), that was measured using a commercial pressure sensor (All sensors 5 psi D1-4V MINI); P was stepped by values of ΔP = 0.5 kPa; (B) close-ups of the data shown in (A); the error, $(3 \times 10^{-4}) \times \Delta R/R_0$, corresponds to 75 Ω error for a 25 kΩ signal.

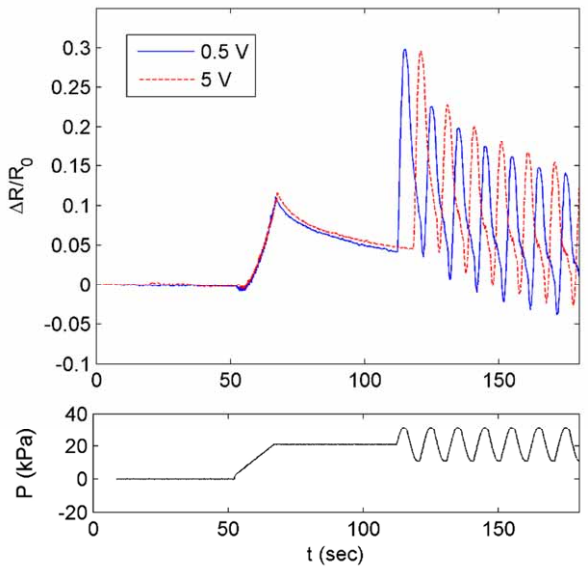

Fig. S5 Source voltage independence of strain sensor signals. Strain sensor signals, $\Delta R/R_0$, that were measured using two different source voltages (0.5 V or 5 V); strain signal amplitudes and relaxation times for both curves are similar; driving pressure, P, is shown in the bottom panel.

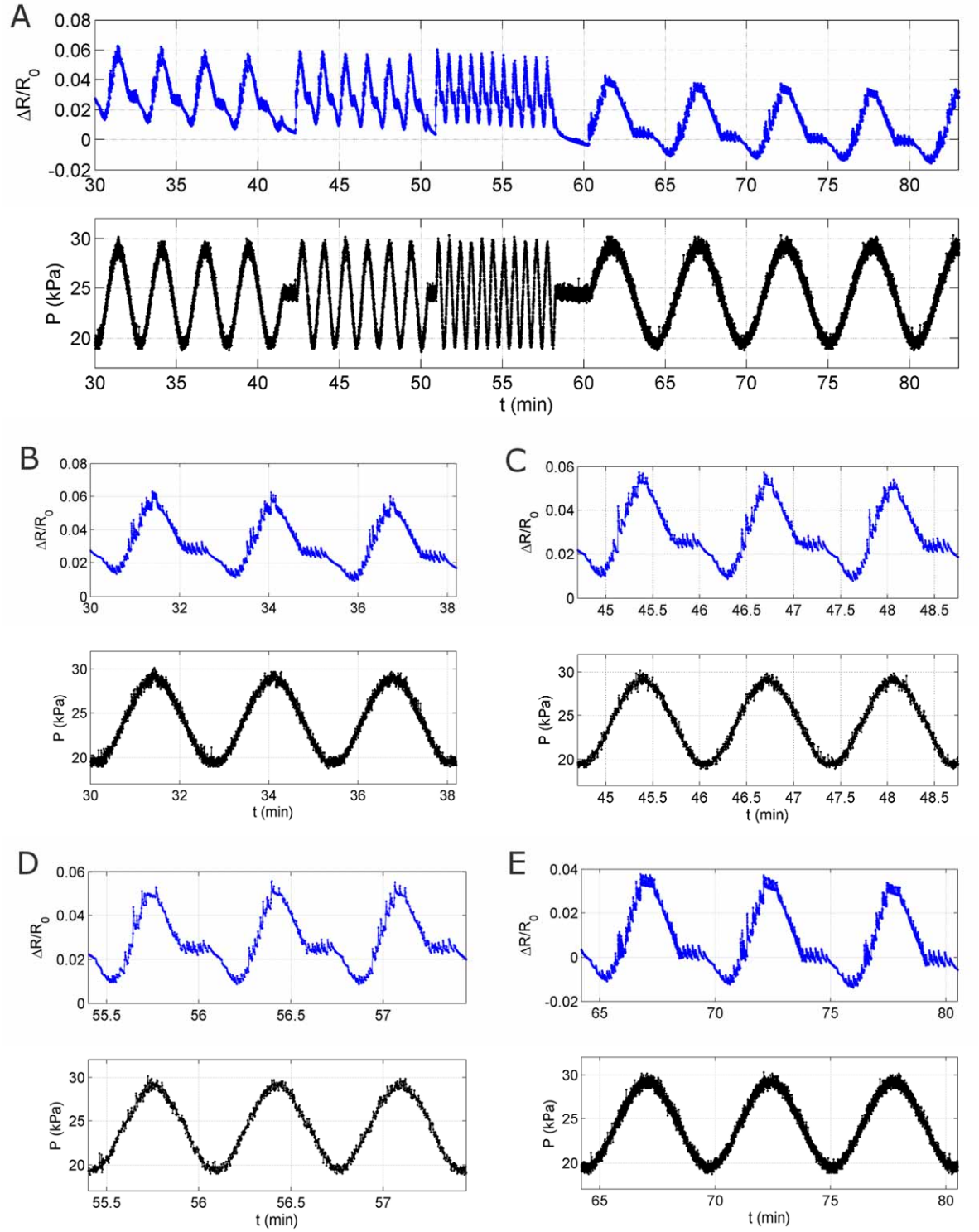

Fig. S6 Strain sensor signals resulting from sinusoidal pressure having several different driving frequencies. (A) Time-dependent resistive strain of a sensor, $\Delta R/R_0$ (top panel), and the corresponding driving pressure, P (bottom panel); (B)-(E) close-ups of various regions within the data shown in (A); Asymmetry of $\Delta R/R_0$ between loading and unloading phases can be seen for all time-scales in (B)-(E).

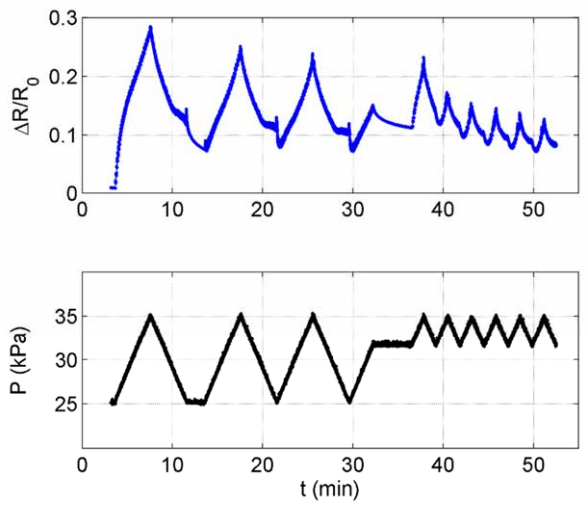

Fig. S7 Strain sensor signal resulting from saw-tooth driving pressure. Time-dependent resistive strain of a sensor, $\Delta R/R_0$ (top panel), and the corresponding driving pressure, P (bottom panel); asymmetry of $\Delta R/R_0$ between loading and unloading phases can be seen.

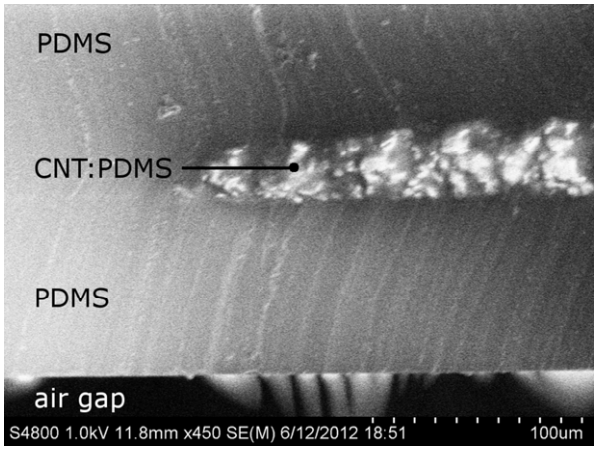

Fig. S8 Scanning electron microscope image of an embedded sensor. The membrane with embedded sensor was cut through the center (region of maximum bulge height) of a conditioned device (number of uses > 20); no delamination of the CNT:PDMS sensor material was observed.

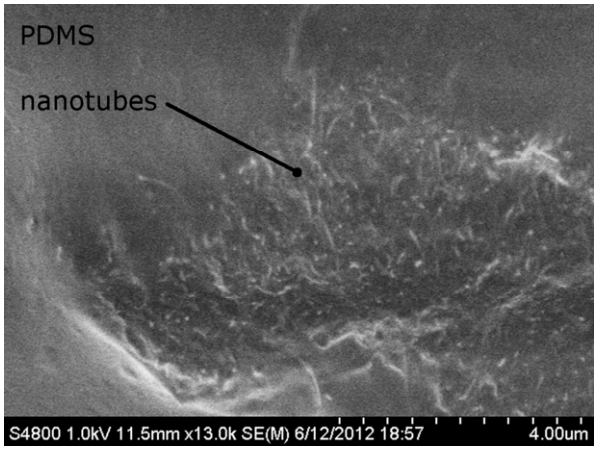

Fig. S9 High-resolution scanning electron microscope (SEM) image of the sensor material. A CNT-rich "pool" similar to those shown in Fig. 5 of the main text is shown above using high-resolution SEM.